

Platelets regulate cell viability and VEGF-A mRNA expression in HaCaT cell line

Abstract

Platelet Rich Plasma (PRP) is an autologous technique that uses centrifuged whole blood to concentrate platelets in plasma. The regenerative effect of PRP is attributed to platelets due to the release of growth factors involved in healing. This study sought to promote the isolation of platelets from PRP (PI-PRP) to identify the role of platelets in the modulation of cell surviving and VEGF-A mRNA expression. The coculture protocol with PI-PRP/keratinocyte cell line HaCaT was established. Cellular viability by MTT, membrane integrity by trypan blue, cell and cytoskeletal cell morphology by DAPI and phalloidin staining and RNA extraction, for subsequently, qRT-PCR VEGF-A, were performed. The MTT test showed higher cell viability in PI-PRP group than CTRL. The trypan blue test showed no difference between CTRL and PI-PRP groups. Fluorescence microscopy analysis showed no changes in cellular morphology of the nucleus and cytoskeleton between groups. In the qRT-PCR the VEGF-A expression was higher in PI-PRP group compared to CTRL. The centrifugation proved to be effective for platelet enrichment. This protocol demonstrated efficiency in studying interaction between platelet and cell lineage.

Keywords: PRP, keratinocyte, platelets, VEGF-A.

INTRODUCTION

Skin tissue contains cells called keratinocytes, which are responsible for cell renewal. When injured, the platelets initiate the healing process through the synthesis of growth factors and the transfer of the molecular information to the target tissue. The most recent studies have opened new paradigms for the functions of platelets, since they show the transfer of messenger RNA (mRNA) and microRNA (miRNA) altering the function of another cell or even activating the production of proteins and the growth factors (Plé 2012; Rowley et al. 2012; Nassa et al. 2017). The synthesis of growth factors and the transfer of molecular information is the principle of cell therapies with stem cells, so the platelets can be framed in this type of cell therapy. Therapies using platelets such as platelet and platelet lysate transplantation have been used for decades (Apatzidou et al. 2021). Autologous plasma treatments in regenerative medicine to optimize the healing process have a lower risk of rejection (Draeos 2019).

The Platelet Rich Plasma (PRP) is the new given to an autologous technique obtained by the process of centrifuging whole blood to obtain the ideal plasma fraction has been proposed to be a therapeutical tool in regenerative medicine to treat some diseases and unaestheticism. The cellular response of proliferation and regeneration in the injured tissue has been correlated with platelets, especially when they reach values four to five times higher than the basal level, reaching up to 1 million platelets/ μ l in PRP (Marx 2004). Variations in the process of obtaining PRP directly affect the result, such as: fresh blood, amount of blood collected, needle gauge for blood collection and plasma transfer, anticoagulants used, number and interval of centrifugations performed, G-force and temperature of the centrifuge (Akhundov et al. 2012). The vast majority of published scientific articles attribute the regenerative effects of PRP to platelets due to the release of growth factors involved in healing vascular endothelium growth factor (VEGF),

epidermal growth factor (EGF), basic fibroblast growth factor (bFGF), platelet-derived growth factor (PDGF) and beta transforming growth factor (TGF- β) however the plasma contains other components hypothetically able to regenerate the skin (Weibrich 2004; Hargrave & Li 2015; Frykberget al. 2010).

Based on the above, the aim of this study is established that allow the isolation of platelets for laboratory tests that can assess the promotion of tissue changes made by the platelets in the skin, especially on keratinocytes, epidermal cells responsible for cell renewal and synthesis of growth factors (McRedmond 2004; Wrzyszc 2017; Wagner 2018; Akhundov 2012; Blanpain & Fuchs 2009; Bae 2015).

MATERIALS AND METHODS

Platelet isolation

This study was approved by the ethics committee (CEP/UFRJ-Macaé 1.922.306). Fifty patients between 18 and 70 years of both sexes, eligible for donation and who agreed to be volunteers, signing the Free Informed Consent Term (FICT) were selected and excluded patients with sexually transmitted infections (STIs), using antihypertensive or acetylsalicylic acid drugs and had a history of cancer.

The isolation of platelets from PRP protocol modified. 6 ml blood was collected from patients with a 22G x 1" needle (25 x 0.7 mm) in a vacuum tube containing Disodium 2,2',2'',2'''-(Ethane-1,2-diyl dinitrilo) tetraacetic acid (EDTA/2Na). The plasma was isolated by centrifugation of the fresh blood at 581x g for 5 minutes. Platelets were isolated from the plasma by centrifugation at 908 x g for 10 minutes. The platelet pellet was suspended in 6 ml DMEM (PI-PRP) (Figure 1). The platelet counts were done using the Rees-Ecker method in the Neubauer chamber, using light microscopy (Aggeler et al.

1946). The number of platelets at coculture per well used was based on the average acquired in platelet counting experiments with the PRP preparation (312,000 platelets/ μ l).

Cell culture

The experimental model was designed for coculture of PI-PRP with the human immortalized keratinocyte cell line - HaCaT, being two experimental groups control - CTRL (HaCaT) and coculture (PI-PRP/HaCaT) (Figure 2). HaCaT cells were maintained in Dulbecco's Modified Eagle's Medium (DMEM - code: D5523, Sigma-Aldrich, Inc.) containing: low glucose, 4 mM L-glutamine, 1 mM sodium pyruvate) supplemented with 1500 mg/L sodium bicarbonate (Scientific Exodus), 4500 mg/L anhydrous glucose (Neon), 100 IU/ml penicillin (Sigma-Aldrich, Inc.), 100 μ g/ml streptomycin (Sigma-Aldrich, Inc.), 250 μ g/ml amphotericin B (Sigma-Aldrich, Inc.) and 10% Fetal Bovine Serum (FBS - Cultilab). The cells were grown, in 25 cm² flasks, with screw cap and filter and sterile (Techno Plastic - TPP, Switzerland) incubated in an incubator COM - 17A6 (Sanyo-biomedical, Japan) at 37°C with a humidified atmosphere containing 5% CO₂.

After approximately 5 to 7 days, they reached 100% confluence and were split in sterile flat-bottom plates (6, 12 or 96 well - TPP, Switzerland). To split the cells, the DMEM were removed, and the cells were washed 2 times with Dulbecco's Phosphate Buffered Saline (D-PBS 1X) without calcium and magnesium and subsequently treated with 1 ml of Trypsin-EDTA solution (Sigma-Aldrich, Inc.) in a CO₂ incubator at 37 °C for 10 minutes. After this time, 4 ml of DMEM was added. Subsequently, the cell suspension was transferred to a 15 ml sterile conical polypropylene tube. Centrifugation was performed in a Centrifuge 80-2B centrifuge (Global Trade

Technology, Brazil) at 327xg for 5 minutes. A precipitate of HaCaT cells was formed and the supernatant discarded. The pellet HaCaT cells were resuspended in 5 ml DMEM. After this step, the cel

1

UNDER PEER REVIEW

suspension was diluted 1:5 and plated in sterile flat-bottom plates (6, 12 or 96 wells) and maintained in a CO₂ incubator at 37 °C until 90% of confluency. Subsequently, the cells were washed twice with D-PBS1X with calcium and magnesium (D-PBS-CM). For cell-starving D-PBS-CM was replaced with DMEM without FBS for 12 to 15 hours in a CO₂ incubator at 37 °C. After a while, the cells were washed twice with D-PBS-CM and the cells were grouped into two experimental groups: CTRL Group: cells cultured in DMEM without FBS. Coculture group: cells cultured with DMEM without FBS + PI-PRP containing 312,000 platelets/μl, for 24 hours in CO₂ incubator at 37 °C. After that, the cells were washed with D-PBS-CM twice for future procedures.

Fluorescence microscopy

The cell morphology was analyzed by fluorescence using dihydrochloric salt, 4',6-diamidino-2-phenylindole (DAPI - Molecular Probes Inc., USA) to stain the nucleus and phalloidin green to stain the cytoskeleton in cells cultured in 12-well plates. After coculture and washing, 500 μl/well of 4% paraformaldehyde (PFA, Vetec Química/Sigma-Aldrich, Inc.) was added for 10 minutes at room temperature (RT) (Shin et al. 2021). Cells from 8 wells were washed twice with D-PBS-CM. 500 μl/well of the solution containing 22.5 μl DAPI (1 mg/ml - Sigma-Aldrich, Inc.) + 45 μl phalloidin green (0.165 μM/ml - Invitrogen) + 4.43 ml D-PBS-CM were added in each well and incubated to 15 minutes on ice protected from light. Cells from 4 wells were washed twice with D-PBS-CM. 500 μl/well of D-PBS-CM were added in each well and incubated for 15 minutes on ice protected from light used for negative control for cell autofluorescence. The plate was taken for analysis by fluorescence optical microscopy in an inverted microscope DMI4

000B(Leica, Germany).

UNDER PEER REVIEW

MTT and Trypan blue Cell viability

Cell viability tests were performed by trypan blue and MTT (Hagio-Izaki et al. 2018; Mosmann 1983). For the trypan blue experiment, was added to the plate 0.5 ml/well of Trypsin-EDTA (Sigma-Aldrich, Inc.) containing adherent cells for 10 minutes in a CO₂ incubator at 37 °C following mixing 0.5 ml/well of DMEM. The cell suspension was transferred to sterile 15 ml polypropylene conical tubes and centrifuged at 327 x g for 5 minutes. The supernatant was discarded, and the cell pellets were suspended in 1 ml of DMEM, 100 µl of cell suspension was mixed to 300 µl of 0.2% trypan blue solution (Sigma-Aldrich, Inc.), and kindly mixed using a micropipette. A 10 µl aliquot was added in a Neubauer chamber. After 2 minutes the number of cells was counted.

For MTT assay (3-[4,5-dimethyl-thiazol-2-yl]-2,5-diphenyltetrazolium), after 24 hours of coculture, the cells were washed twice with D-PBS-CM supplemented with 5 mM of glucose (D-PBS-CMG). 200 µl of the 0.1% MTT solution (Sigma-Aldrich, Inc.) in D-PBS-CMG was added in each well of the 96-well plate and incubated for 2 hours in a CO₂ incubator at 37°C. Then, the plates were kept on ice where they were washed twice with D-PBS-CMG. 200 µl of dimethyl sulfoxide (DMSO, Sigma-Aldrich, Inc) were added for 5 minutes in Kline NT151 shaker (Novatecnica, Brazil). The results were read in a microplate reader Thermo Plate (Thermo Fisher Scientific, USA) with a wavelength of 540 nm.

RNA extraction and real time PCR

The RNA was extracted from the cells using Trizol® (Invitrogen, Carlsbad, CA, USA) following manufacture's instructions. RNA quantification was performed on a NanoDrop® 2000c spectrophotometer (Thermo Fisher Scientific, USA) with readings

at 260 nm and 280 nm. When necessary due to the presence of genomic DNA, RNA samples

UNDER PEER REVIEW

were treated with the DNase (Turbo DNA-free® kit, Invitrogen, USA) following the manufacturer's instructions. VEGF-A gene expression was performed after washing the plate in coculture, by extracting the RNA using the method with adaptations. The primers for VEGF-A and β -actin (used as gene reference) amplification were designed using NCBI Primer Blast (<http://www.ncbi.nlm.nih.gov>) and Clustal omega (www.clustal.org) software using the following criteria: 18 and 24 nucleotides in different exons, maintaining a melting temperature or T_M (melting temperature) of $60^\circ\text{C} \pm 1^\circ\text{C}$ and with a guanine-cytosine (GC) content ratio of 45 to 60 % and product amplification size up to 150 bp.

Complementary DNA (cDNA) synthesis was performed using the High-Capacity cDNA Reverse Transcription kit (Applied Biosystems, USA), following the manufacturer's instructions. The mRNA content was amplified using the conventional PCR technique with the GoTaq® G2 Colorless Master Mix kit (Promega Corporation, USA), according to the manufacturer's guidelines, using the specific primer pairs designed for this study (Table 1). This step was performed to certify that the amplification product generated in the reaction was the same size as that predicted. After confirming the size of the amplification product, the mRNA content of VEGF-A and β -Actin was determined by the real-time PCR technique (qRT-PCR) using the SYBR Green kit (Applied Biosystems, USA) on a RealTime StepOne Plus® (Applied Biosystems, USA), according to the manufacturer's instructions. Transcriptional levels were normalized using the β -actin gene. The relative expression was calculated from the mean \pm SEM values of $2^{-(\Delta\Delta C_t)}$ (Livak & Schmittgen 2021).

Statistical Analyses

The results were expressed as mean \pm SEM. The Shapiro-Wilk test was used to assess whether each sample group had a normal distribution. Confirming the normal distribution, significance was determined using the One-Way ANOVA unpaired test with Bonferroni post-test for experiments with 3 or more experimental groups (Ghasemi & Zahediasl 2012). The Student T test was used for experiments with only two experimental groups. Differences were considered significant with $p < 0.05$. Analyses were performed using the GraphPad Prism 4 program (GraphPad Software, Inc).

RESULTS

Platelet isolation and enrichment

The PRP was prepared with adaptations made in this study to obtain the PI-PRP (Figure 1). The precipitate of platelets was obtained (Figure 3A). The observation of PI-PRP in Neubauer chamber using optical microscopy shows significant enrichment of platelets and rare red blood cells present (Figure 3B). The platelet count (platelet/ μ l) in PI-PRP was higher than in whole blood ($474,500 \pm 74,506$ and $312,250 \pm 43,014$; $n = 4$; $p < 0.05$; respectively) (Figure 3C). The times of platelet enrichment were approximately 2.3 in PI-PRP compared to whole blood (2.28 ± 0.43 and 1.00 ± 0.00 ; $n = 6$; $p < 0.05$; respectively) (Figure 3D).

Cell morphology under fluorescence microscopy

To ascertain whether platelets can induce changes in the nuclear and cytoskeletal morphology of HaCaT cells, cellular labeling with DAPI and phalloidin fluorophores was conducted. Upon examination under fluorescence microscopy, there were no significant changes observed in nuclear morphology following coculture treatment; however, distinct alterations in cytoskeletal organization were noted. (Figure 4).

Cell viability

To verify if platelets can induce changes in the viability of HaCaT cells, cell viability tests were performed by trypan blue and MTT. The Trypan blue test showed no significant difference in cell number (cells/ml) between coculture group ($540,000 \pm 89,019$; $n=9$; $p > 0.05$) and CTRL group ($531,667 \pm 76,879$ $n = 9$) (Figure 5A). In the MTT test it was possible to observe higher cell viability (times the CTRL) in the coculture group (1.18 ± 0.09 , $n= 11$) compared to the CTRL group (1.00 ± 0.00 , $n = 15$, $p < 0,05$) (Figure 5B).

VEGF-A mRNA expression

In the qRT-PCR the VEGF-A expression (times the CTRL) was higher in the coculture group (4.61 ± 1.85 ; $n=6$; $p < 0.05$) compared to the CTRL group (1.00 ± 0.00 ; $n=9$) (Figure 6).

DISCUSSION

This protocol performed in an analogic centrifuge, common in clinics and offices, using a lowervolume of whole blood when compared to the protocol performed by McRedmond et al. (2004) and Wryszcz et al. (2017) who used 50 ml and 10 ml, respectively, of blood and was effective in concentrating and purifying the platelets obtained from PRP. Despite the red coloration of the formed precipitate, the presence of red blood cells was minimally identified by optical microscopy in a Neubauer chamber, demonstrating a level of purity achieved in the method.

Once concentrated and purified in PI-PRP, the platelets could be used as an experimental model in coculture studies with HaCaT cells. Engebretsen et al. (2010) advocates the isolation of platelets for laboratory purposes.

Cellular damage to HaCaT was not observed; we can question whether the therapeutic use of purified platelets would be more appropriate due to the reduction of interfering factors. No studies were found in the literature for the use of platelet precipitates or their suspension for therapeutic purposes.

The analysis of cellular morphology of the nucleus and cytoskeleton through fluorescence microscopy revealed no evidence of morphological changes in the nucleus of HaCaT cells, but exhibited alterations in cytoskeletal organization. This data suggests that cells under co-culture with platelets adopt a different morphology, yet this change is not associated with a decrease in cell viability (Han et al., 2007). Further supporting this hypothesis is the significant increase in mitochondrial activity observed in the coculture, as evidenced by the MTT assay. These findings imply an enhancement in cell viability following treatment with PI-PRP (Zheng et al., 2016).

Future studies are needed to verify whether PI-PRP increases the cellular oxygenation of keratinocytes, a mechanism to be explored for the use of PI-PRP in alopecia. In studies on the use of PRP for the treatment of alopecia, vascular mechanisms are attributed, as being caused by the increase in vascular structures around hair follicles and angiogenesis, as a response to the anti-hair loss action found (El Taieb et al. 2017). Once the VEGF-A is involved in angiogenesis, this growth factor can be an important player in the endothelial growth promoting improvement in follicular oxygenation and reducing hair loss in alopecia. In this study it was observed that the PI-PRP was able to increase VEGF-A mRNA content in HaCaT cells, suggesting that platelets could be able to increase vascular proliferation and oxygenation of keratinocytes. This upregulation in VEGF-A mRNA may be an effect of platelet adhesion to keratinocytes. Thus, it would be interesting for future studies with platelets to identify the cellular and molecular mechanisms involved

in the improvement of cellular viability and upregulation of VEGF-A in keratinocytes cells.

CONCLUSION

In this study was able to standardize a new protocol for platelet isolation from small samples of peripheral blood. Also, it was observed that PI-PRP seems to be harmless for HaCaT cell lines and promotes improvement in cell proliferation and VEGF-A mRNA expression. For the first time, this study developed a feasible protocol to study the interaction between platelets and target cells.

CONFLICT OF INTERESTS

The authors of this study do not have professional relationships with companies or manufacturers who will benefit from the results of the present study.

The results of the present study do not constitute an endorsement by the ACSM.

The authors of this study declare that the results are presented clearly, honestly, and without fabrication, falsification, or inappropriate data manipulation.

Consent

As per international standards or university standards, patient(s) written consent has been collected and preserved by the author(s).

Ethical approval: This study was approved by the ethics committee (CEP/UFRJ-Macaé 1.922.306).

REFERENCES

AGGELERPM, HOWARDJ, LUCIASP & MILLS, E. 1946. Platelet counts and platelet function. *Blood* 1(6):472–496. doi: 10.1182/blood.V1.6.472.472.

UNDER PEER REVIEW

AKHUNDOVK, PIETRAMAGGIORIG, WASELLEL, DARWICHES, GUERIDS, SCALETTAC, HIRT-BURRIN, APLEGATELA & RAFFOUL WV. 2012.

Development of a cost-effective method for platelet-rich plasma (PRP) preparation for topical wound healing. *Annals of Burns and Fire Disasters* 25(4):207–213. PMID:23766756 PMCID: PMC3664531.

AKHUNDOV K, PIETRAMAGGIORI G, WASELLE L, DARWICHE S, GUERID S, SCALETTAC, HIRT-BURRIN, APLEGATELA & RAFFOUL WV. 2012.

Development of a cost-effective method for platelet-rich plasma (PRP) preparation for topical wound healing. *Ann Burns Fire Disasters* 25(4):207-213.

APATZIDOUDA, BAKOPOULOU AA, KOUZI-KOLIAKOU K, KARAGIANNIS V & KONSTANTINIDIS A. 2021. A tissue-

engineered biocomplex for periodontal reconstruction. A proof-of-principle randomized clinical study. *J Clin Periodontol* 48(8):1111-1125. doi:10.1111/jcpe.13474.

BAE ON, NOH M, CHUN YJ & JEONG TC. 2015. Keratinocytic Vascular Endothelial Growth Factor as a Novel Biomarker for Pathological Skin Condition. *Biomol Ther* 23(1):12–18. doi:10.4062/biomolther.2014.102.

BLANPAIN C & FUCHS E. 2009. Epidermal homeostasis: a balancing act of stem cells in the skin. *Nat Rev Mol Cell Biol* 10(3):207-217. doi: 10.1038/nrm2636.

DRAELOSZD, RHEINSLA, WOOTTENS, KELLARRS & DILLERRB. 2019. Pilot study: Autologous platelet-rich plasma used in a topical cream for facial rejuvenation. *J Cosmet Dermatol* 18(5):1348-1352. doi:10.1111/jocd.13088.

ELTAIEBMA, IBRAHIMHM, NADAE & SEIFAL-DINM. 2017. Platelet-rich plasma versus minoxidil 5% in treatment of alopecia areata: A trichoscopic evaluation. *Dermatol Ther* 30(1). doi:10.1111/dth.12437.

ENGBRETSEN ET AL. 2010. IOC consensus paper on the use of platelet-rich plasma in sports medicine. *Br J Sports Med* 44(15):1072-1081. doi:10.1136/bjism.2010.079822. FRYKBERG RG, DRIVER VR, CARMAND, LUCEROB, BORRIS-HALEC, FYLLING CP, RAPPL LM & CLAUSEN PA. 2012. Chronic wounds treated with a physiologically relevant concentration of platelet-rich plasma gel: a prospective case series. *Ostomy Wound Manage* 56(6):36-44. GHASEMI A & ZAHEDIASL S. 2012. Normality tests for statistical analysis: a guide for non-statisticians. *Int J Endocrinol Metab* 10(2):486-489. doi:10.5812/ijem.3505. HAGIO-IZAKIK, YASUNAGAM, YAMAGUCHI M, KAJIYAH, MORITAH, YONEDA M, HIROFUJI T & OHNO J. 2018. Lipopolysaccharide induces bacterial autophagy in epithelial keratinocytes of the gingival sulcus. *BMCCell Biol* 19(1):18. doi:10.1186/s12860-018-0168-x. HANJ, MENGHX, TANGJM, LISL, TANGY & CHENZB. 2007. The effect of different platelet-rich plasma concentrations on proliferation and differentiation of human periodontal ligament cells in vitro. *Cell Prolif* 40(2):241-252. doi:10.1111/j.1365-2184.2007.00430.x. HARGRAVE B & LI F. 2015. Nanosecond Pulse Electric Field Activated-Platelet Rich Plasma Enhances the Return of Blood Flow to Large and Ischemic Wounds in a Rabbit Model. *Physiol Rep* 3(7):e12461. doi:10.14814/phy2.12461. LIVAKKJ & SCHMITTGENTD. 2001. Analysis of relative gene expression data using real-time quantitative PCR and the 2⁻(-Delta Delta C(T)) Method. *Methods* 25(4):402-408. doi:10.1006/meth.2001.1262. MARX RE. 2004. Platelet-rich plasma: evidence to support its use. *J Oral Maxillofac Surg* 62(4):489-496. doi:10.1016/j.joms.2003.12.003.

MCREDMONDJP,PARKSD,REILLYDF,COPPINGERJA,MAGUIREP,
SHIELDS DC & FITZGERALD DJ. 2004. Integration of proteomics and genomics
in platelets: a profile of platelet proteins and platelet-specific genes. *Mol Cell
Proteomics*3(2):133-144.doi:10.1074/mcp.M300063-MCP200.

MOSMAN NT. 1983. Rapid colorimetric assay for cell growth and survival: Application
to proliferation and cytotoxicity assays. *J Immunol Methods* 65(1-2):55-
63.doi:10.1016/0022-1759(83)90303-4.

NASSA G ET AL. 2018. Splicing of platelet resident pre-mRNAs upon activation
by physiological stimuli results in functionally relevant proteome modifications. *Sci
Rep*8(1):498.doi:10.1038/s41598-017-18985-5.

PLÉH, LANDRY P, BENHAMA, COARFAC, GUNARATNEP & PROVOST P.
2012. The repertoire and features of human platelet microRNAs. *PLoS One*7(12):e50746.doi:
10.1371/journal.pone.0050746.

ROWLEY JW, OLERAJ, TOLLEY ND, HUNTER BN, LOWEN, NIX DA, YOST CC,
ZIMMER MANGA & WEYRICH AS. 2011. Genome-wide RNA-
seq analysis of human and mouse platelet transcriptomes. *Blood* 118(14):e101-
11.doi:10.1182/blood-2011-03-339705.

SHIN H, CHOI JH & LEE JY. 2021. Probing TGF- β 1-
induced cytoskeletal rearrangement by fluorescent-
labeled silicic acid nanoparticle uptake assay. *Biochem Biophys Res Commun*. 2021;28:101137.
doi:10.1016/j.bbrep.2021.101137.

WAGNER T, GSCHWANDTNER M, STRAJER IUA, ELBE-
BÜRGER A, GRILLARI J, GRILLARI-
VOGLAUER R, GREINER G, GOLABIB, TSCHACHLER E &
MILDNER M. 2018. Establishment of keratinocyte cell lines from human hair
follicles. *Sci Rep*8(1):13434. doi:10.1038/s41598-018-31829-0.

WEIBRICHG,HANSENT,KLEISW,BUCHR&HITZLERWE.2004.Effectof
platelet concentration in platelet-rich plasma on peri-implant bone regeneration.
Bone34(4):665-671.doi:10.1016/j.bone.2003.12.010.

WRZYSZCZA,URBANIAKJ,SAPAA&WOŹNIAKM.2017.Anefficientmethod
for isolation of representative and contamination-free population of blood platelets
forproteomic studies.Platelets28(1):43-53.doi:10.1080/09537104.2016.1209478.

ZHENG C,ZHU Q,LIU X,HUANG X,HE C,JIANG L,QUAN D,ZHOU X&ZHU
Z.2016.Effectofplatelet-
rich plasma (PRP) concentration on proliferation, neurotrophic function and migration of
Schwann cells in vitro. J Tissue Eng Regen Med 10(5):428-436.doi:10.1002/term.1756.

FIGURE'S LEGENDS

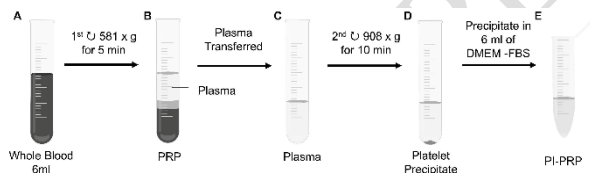


Figure 1

Experimental design of platelet isolation from PRP to obtain PI-PRP. (1a) 6 ml of blood were collected with a 22G x 1" needle (25 x 0.7 mm) in vacuum tube containing EDTA Na+2. (1b) Whole blood was centrifuged at 581 x g for 5 minutes and the plasma was collected and (1c) transferred to a new tube. (1d) A second centrifugation was performed at 908 x g for 10 minutes to obtain the platelet precipitate. The supernatant was discarded. (1e) The platelet precipitate was resuspended in 6 ml of DMEM without fetal bovine serum (DMEM-FBS), being called isolated platelet precipitate suspension (PI-PRP).

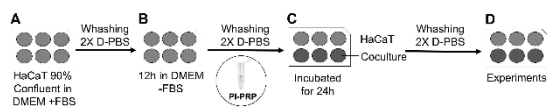


Figure 2

HaCaT/PI-

PRP coculture assay. (2a) After reaching confluence, around 48 to 72 hours in culture, the HaCaT cells were splitted in a 6-

well plates in DMEM with 10% Fetal Bovine Serum (DMEM+FBS) and incubated in an oven with 5% CO₂ at 37°C until 90%

confluence. (2b) The cells were washed twice with Dulbecco's Phosphate-

Buffered Saline solution (D-PBS 1X with calcium and magnesium) and 2 ml of DMEM without FBS (DMEM -FBS) was added to each well and incubated for 12 hours in

incubator with 5% CO₂ at 37°C. (2c) The HaCaT was washed twice with D-PBS 1X with calcium

and magnesium. Half of the wells (in light gray) received 2 ml/well of DMEM without FBS (DMEM-FBS) being HaCaT group. The other wells (in dark gray) were cocultured with isolated

platelet precipitate suspension (PI-PRP 312,000 platelets/ μ l of DMEM -FBS final volume of 2 ml). being Coculture group. HaCaT and Coculture groups

were incubated for 24 hours in 5% CO₂ atmosphere incubator at 37°C. (2d) The experimental groups were washed again twice with D-PBS 1X with calcium and

magnesium to carry out the study experiments.

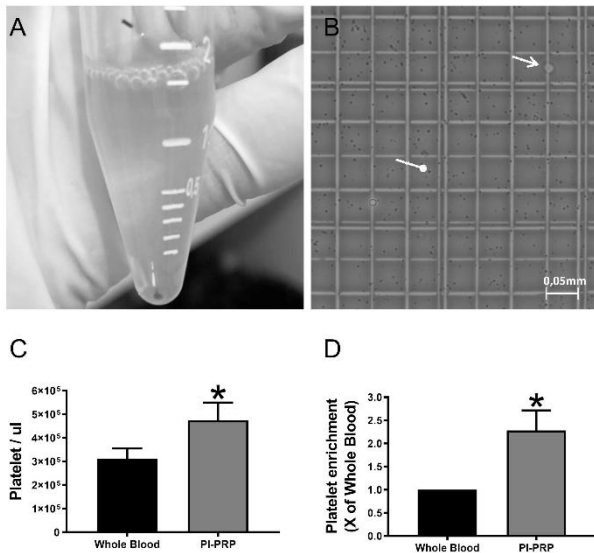


Figure 3

Platelet counting in PI-PRP. (3a) representative image of the precipitate platelets indicated by the black arrow. (3b) representative image showing PI-PRP in Neubauer chamber. The platelets are indicated by arrow with arrowhead and the red blood cells are reindicated by round tip arrow. The platelets were stained by Rees-Ecker method and analyzed by optical microscopy with phase contrast at 200X magnification in a Neubauer chamber. (3c) Graphic representation of platelet counting in whole blood and PI-PRP. (3d) Graphic representation of the platelet enrichment in PI-PRP compared to whole blood. Values are represented as Mean \pm SEM, n=5, (*) indicates $p < 0.05$.

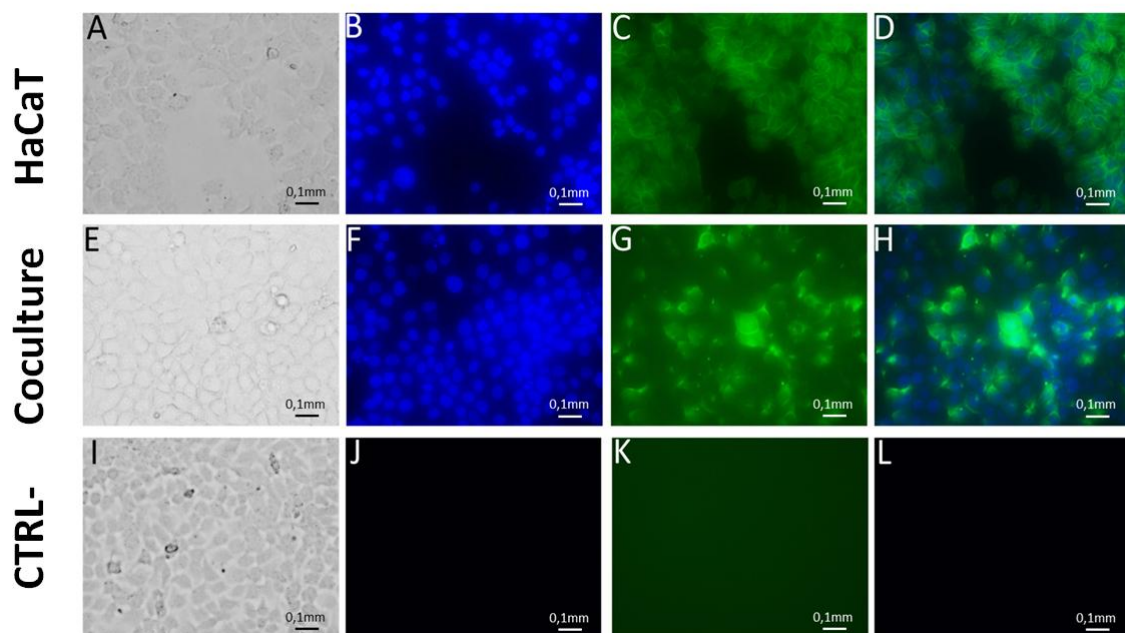


Figure 4

Fluorescence optical photomicrography of HaCaT and PI-PRP coculture. The images were obtained using an inverted microscope with a magnification of 400X and a scale of 0.1mm. Where (4a) HaCaT, (4b) HaCaT showing the nucleus stained by DAPI, (4c) HaCaT showing the cytoskeleton stained by phalloidin green, (4d) HaCaT overlapping DAPI /Phalloidin. (4e) Coculture HaCaT and PI-PRP (HaCaT/PI-PRP). (4f) HaCaT/PI - PRP showing the nucleus stained by DAPI, (4g) HaCaT/PI-PRP by fluorescence showing the cytoskeleton stained by phalloidin green, (4h) HaCaT/PI-PRP overlapping DAPI/Phalloidin. (4i) HaCaT without any staining. (4j) Cells of panel I visualized in DAPI filter showing no background fluorescence. (4k) Cells of panel I visualized in phalloidin green filter showing no background fluorescence. (4l) Overlapping of the images from panels 4j and 4k.

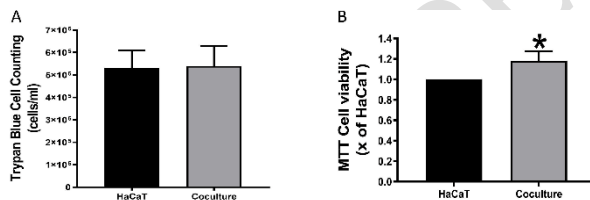


Figure 5

Cell viability accessed by trypan blue staining and MTT. (5a) Graphic representation of trypan blue cell counting. The graph represents the cell counts of the HaCaT group and coculture group showing no significant difference between both groups. Values are represented as Mean \pm SEM, n=9. (5b) Graphic representation of MTT cell viability. The graph shows results from the two groups HaCaT and coculture showing a significant difference between both groups. Values are represented as Mean \pm SEM, n = 11, (*) indicates $p < 0.05$.

	Forward 5'-3'	Reverse 5'-3'	Produ	Reference
--	---------------	---------------	-------	-----------

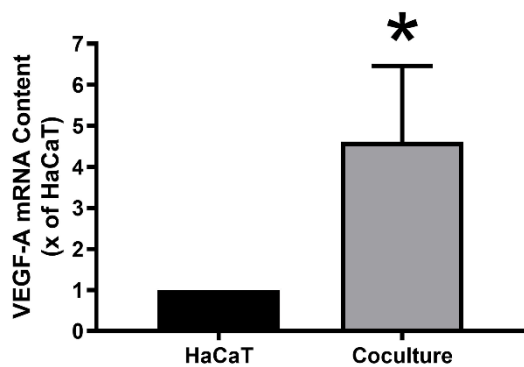


Figure 6

Graphic representation of relative VEGF-

A mRNA content in HaCaT and in coculture groups. Real Time PCR showing that relative

VEGF-A mRNA content in Coculture

is higher than HaCaT group. Values are represented as Mean \pm SEM, n=8, (*) indicates $p < 0.05$.

			ct size	sequence
VEG	ctctacctccaccatgcca	tcgtgatgattctgccctc	71 bp	NM_001025366
F-A	ag	ct		.3
β-actin	cctcgccttgccgatcc	cgcggggatatcatcatc	70 bp	NM_001101.5
		cat		

Table 1. The primer pairs used for amplification of VEGF-A and β-actin mRNAs.

UNDER PEER REVIEW